
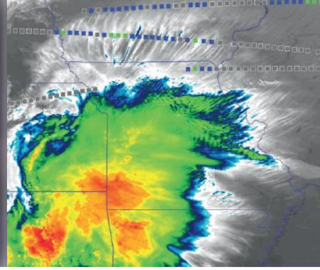

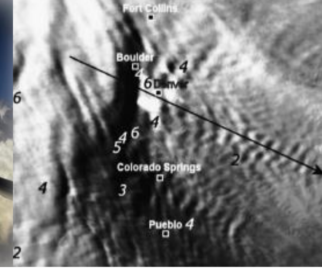


Atmospheric Turbulence Estimation using High Vertical-Resolution Radiosonde Data (HVRRD) in USA: Application to Aviation Turbulence

Hye-Yeong Chun and Han-Chang Ko

Department of Atmospheric Sciences, Yonsei University, Seoul, Korea

Acknowledgement: *Robert Sharman at NCAR, USA*

Outline

- Introduction
- Thorpe's method and data
- Characteristics and potential sources of the estimated turbulence in the troposphere and stratosphere (Ko and Chun 2021, AR)
- Comparison with in-situ flight EDR (Ko et al. 2021, preparation)
- Summary

Introduction

- **Atmospheric turbulence** plays an important role in **momentum and energy exchanges between different scales of atmospheric motions**.
- Understanding the atmospheric turbulence is a considerable **challenge due to the localized, intermittent, and sporadic nature of turbulence** (Kim, 1991; Clayson and Kantha, 2008; Muhsin et al., 2016; Kohma et al., 2019).
- **Observational turbulence studies in the free atmosphere** have mainly been conducted using **radar, aircraft, and rocket** observations (Hocking, 1988; Lübken, 1992; Nastrom and Eaton, 1997; Cho et al., 2003; Singh et al., 2008; Dehghan et al., 2014; Sharman et al., 2014), although **geographical coverage of those instruments is limited**.
- Recently, turbulence estimation based on the **Thorpe method** (Thorpe, 1977) using **operational high vertical resolution radiosonde data (HVRRD), with 1 second resolution**, has been conducted over **vast regions for long periods** (Clayson and Kantha, 2008; Alappattu and Kunhikrishnan, 2010; Nath et al., 2010; Kantha and Hocking, 2011; Love and Geller, 2012; Schneider et al., 2015; Sunilkumar et al., 2015; Li et al., 2016; Muhsin et al., 2016; Sun et al., 2016; Bellenger et al., 2017; Zhou et al., 2018; Ko et al., 2019; Kohma et al., 2019; Zhang et al., 2019; He et al., 2020; Muhsin et al., 2020; Geller et al., 2021).

Maximum number of levels per BUFR radiosonde report (Dec. 2015)

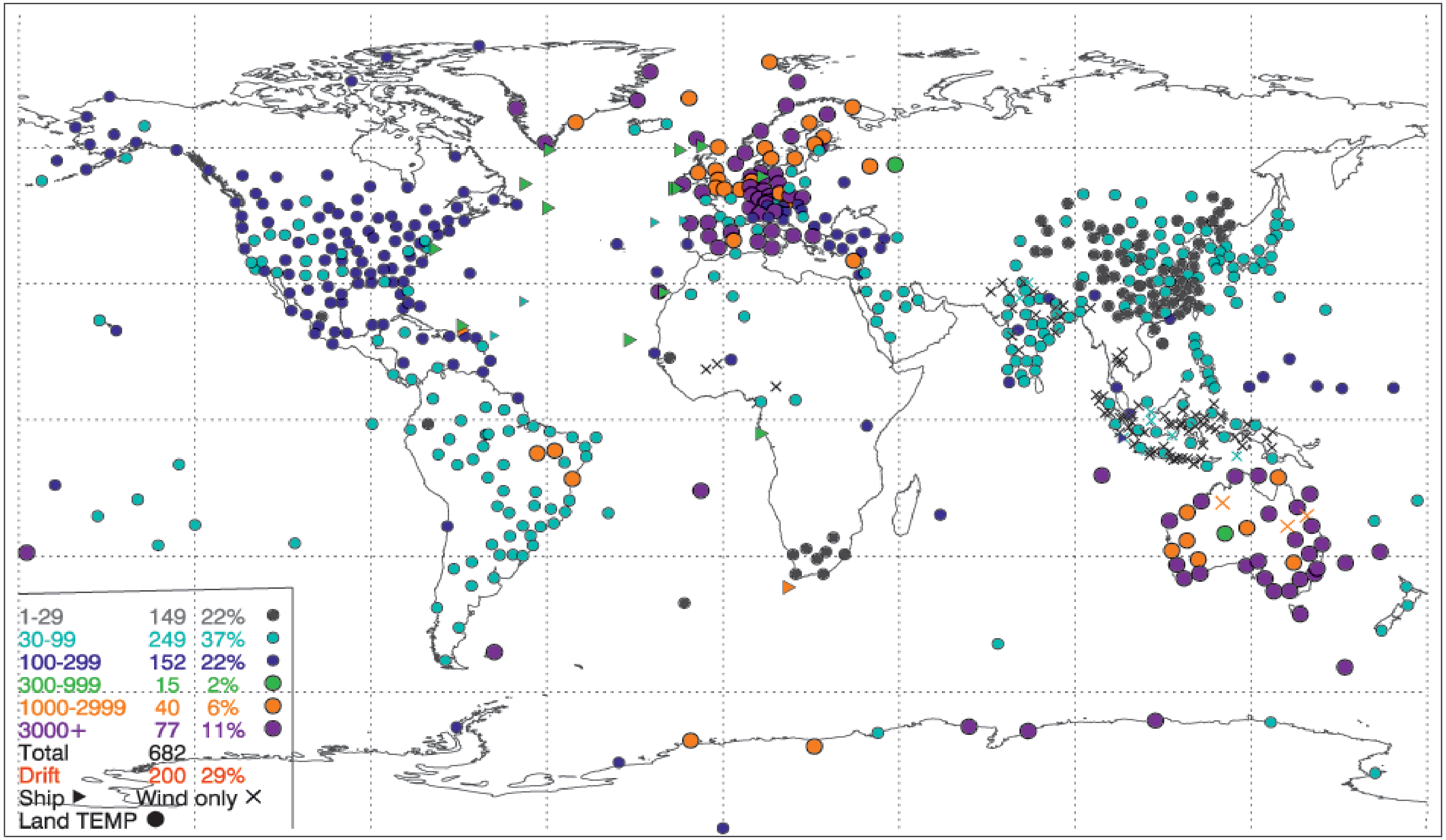

Ingleby et al. (2016, BAMS)

Method (Thorpe's Method)

"Resorting" (Thorpe 1977)

Red: observed potential temperature
Blue: resorted potential temperature

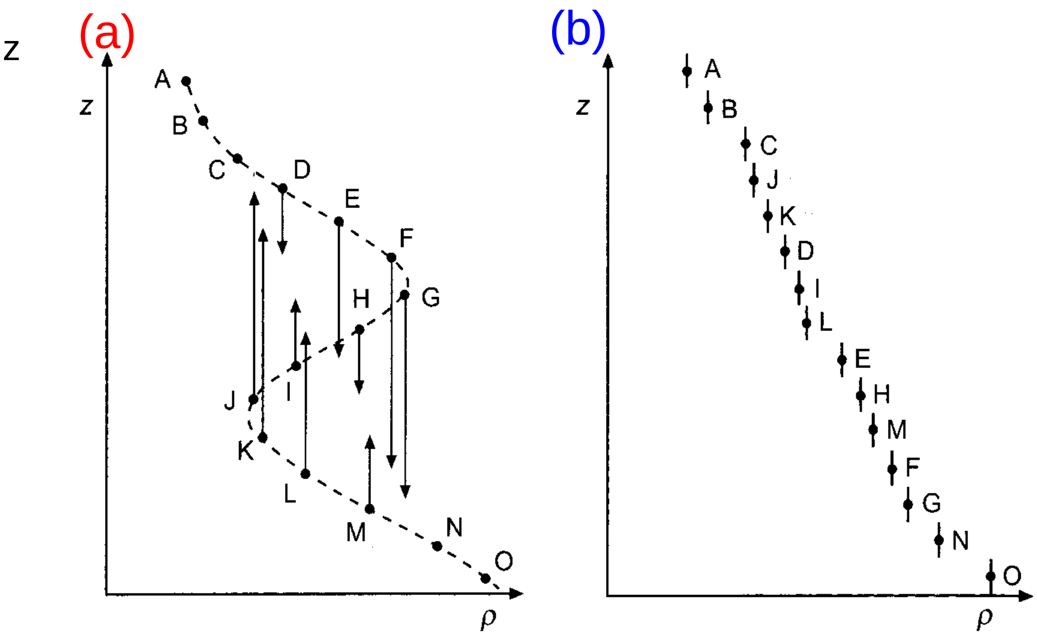

Observed density profile

Resorted density profile

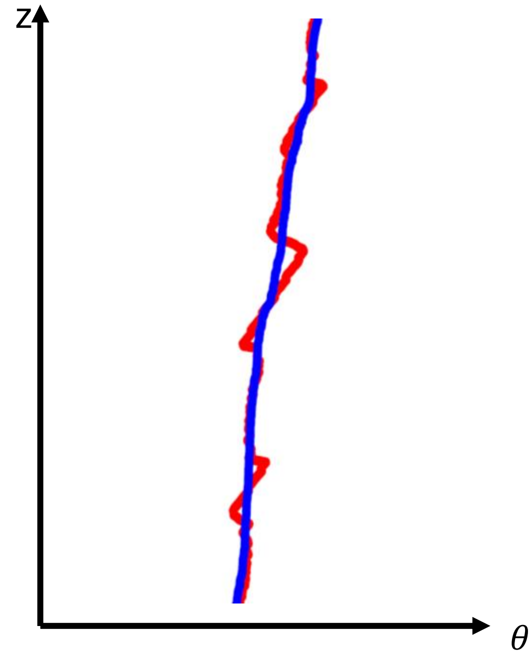

- The observed profile of density (a) is vertically displaced by turbulent motion, from (b) a basic stable profile without time for significant molecular diffusion to occur.
- In the atmosphere, potential temperature can be used (Clayson and Kantha, 2008).
- This method is applied to the free atmosphere

Estimation of eddy dissipation rate using Thorpe's method

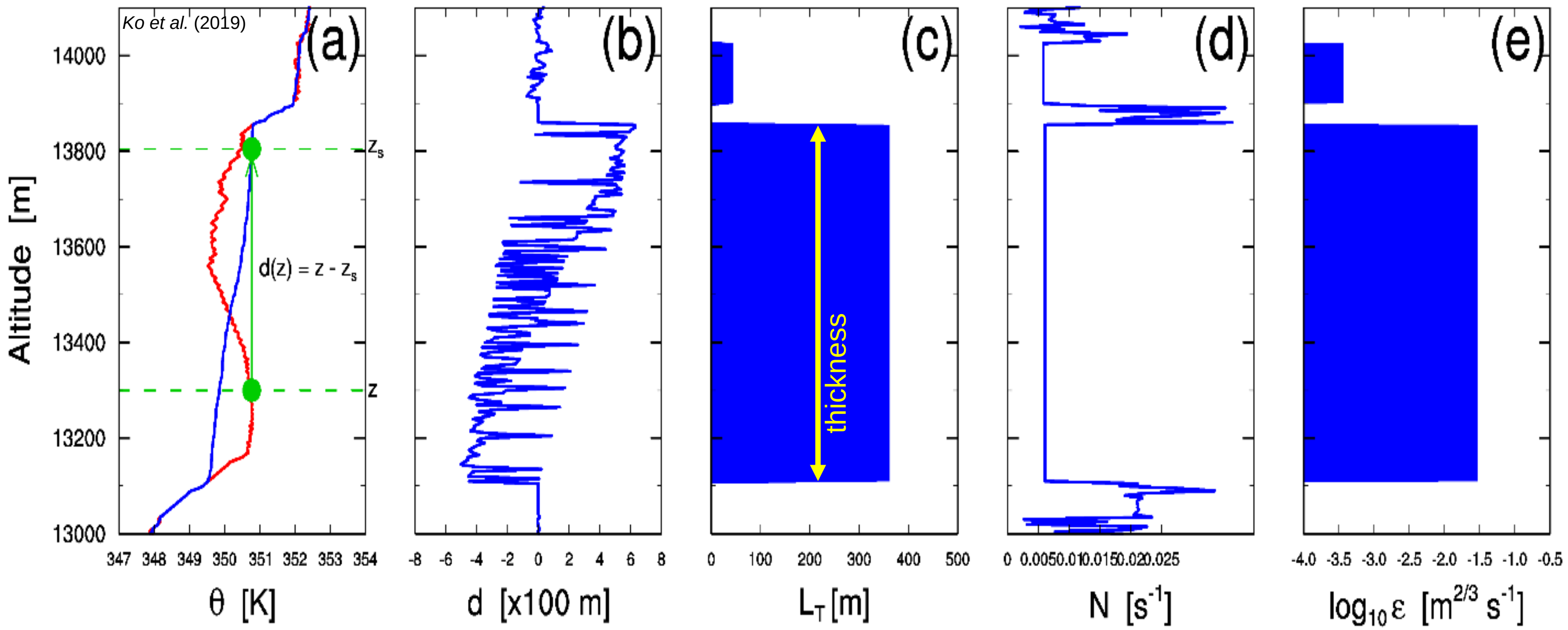

red: observed θ

blue: stably sorted θ

- $d = z - z_s$ is defined as Thorpe displacement, and whose root-mean-square (rms) value in detected turbulent layer is Thorpe scale (L_T).
- Thorpe scale is linearly correlated with the Ozmidov scale [$L_o \equiv (\varepsilon/N^3)^{1/2}$)].

  Using $L_o = cL_T$,

$$\boxed{\varepsilon = C_K {L_T}^2 N^3 \text{ where } C_K = c^2.}$$

C_K=0.3: Clayson and Kantha (2008)

C_K=1.0: Kantha and Hocking (2011), Li et al. (2016)

Data

Ko and Chun (2021, AR)

	Operational high vertical-resolution radiosonde data (HVRRD)
No. of stations	68
Resolution	1 s (~5 m vertically)
Observations	P, T, Rh, U, V, z
Launch frequency	twice a day (00 and 12 UTC)
Data period	Jan. 2012-Dec. 2017 (6 years)

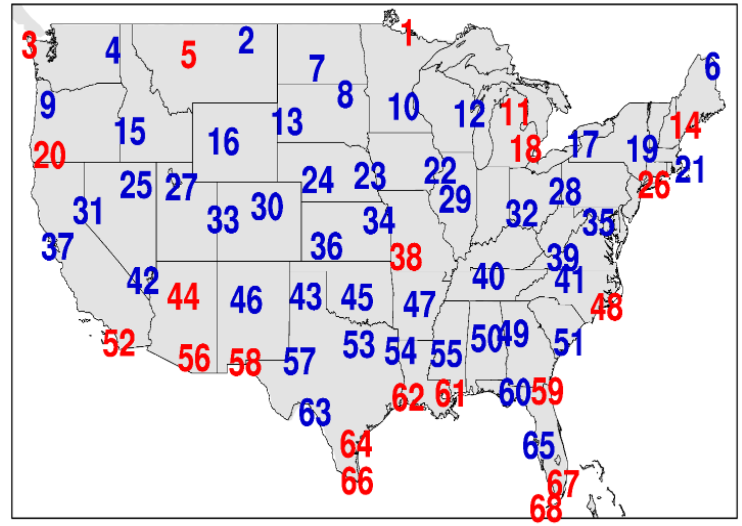

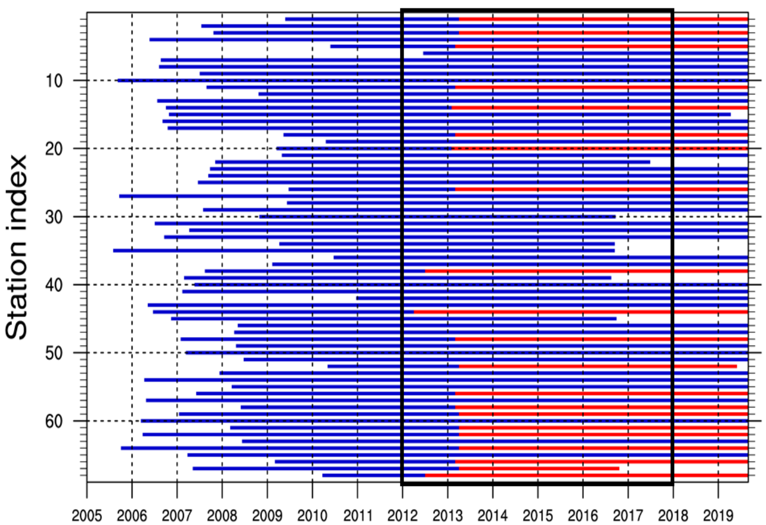

blue: Lockheed Martin LMS-MkIIa: **212,023** profiles
red: Väisälä RS92-NGP: **72,378** profiles

As the transition of radiosonde instruments can significantly affect the turbulence estimation (**Geller et al. 2021, MWR**), we used the data exclusively from the Lockheed Martin LMS-MkIIa.

Monthly occurrence frequency of unstable layers of thickness 10-400 km (z=15-25 km)

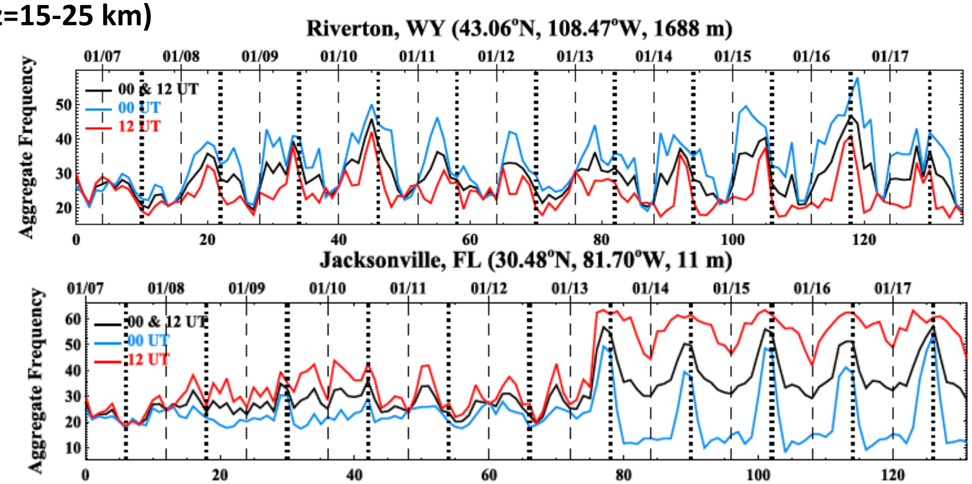

Geller et al. (2021, MWR)

Characteristics of turbulence retrieved from HVRRD

Troposphere(TR): 3km-tropopause

Stratosphere(ST): tropopause-30km

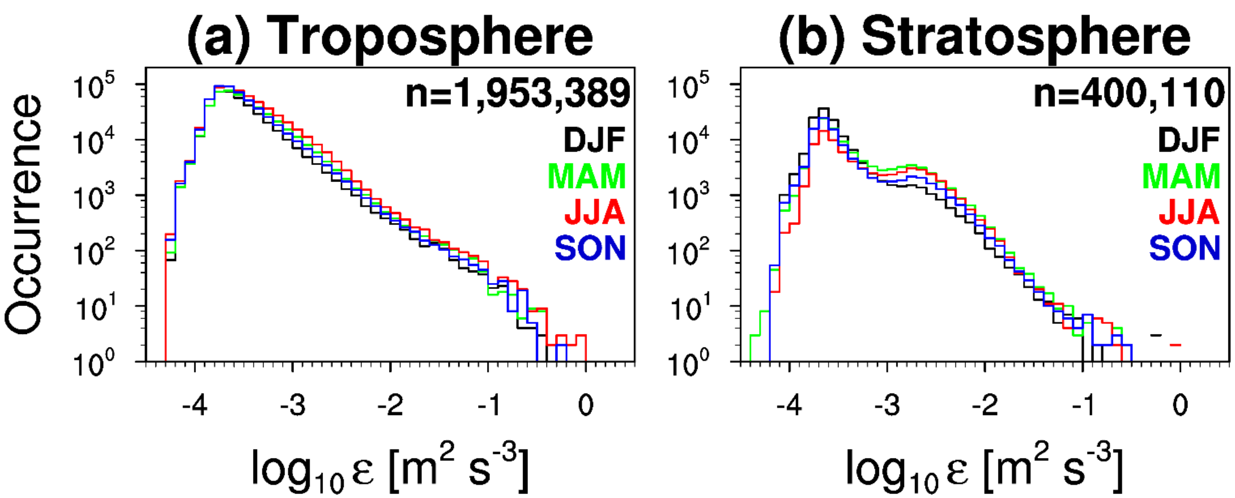

- More strong turbulence ($\log_{10}\varepsilon$>-3 m^2 s^{-3}) in TR than in ST.
- Largest in JJA in TR, less evident in ST

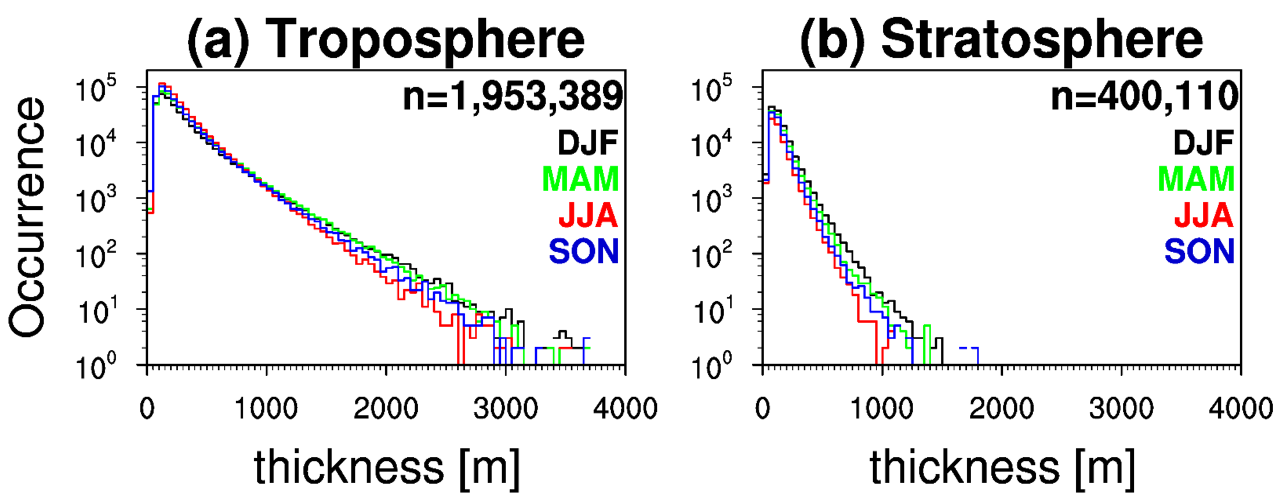

- Mean(median) thickness is 278(205)m in TR and 140(115) in ST.
- Largest in JJA for small thickness (<1000m) and in DJF for large thickness (>1000m) in TR, and largest in DJF in ST

Horizontal distributions of layer-mean thickness of turbulence layer (THTL)

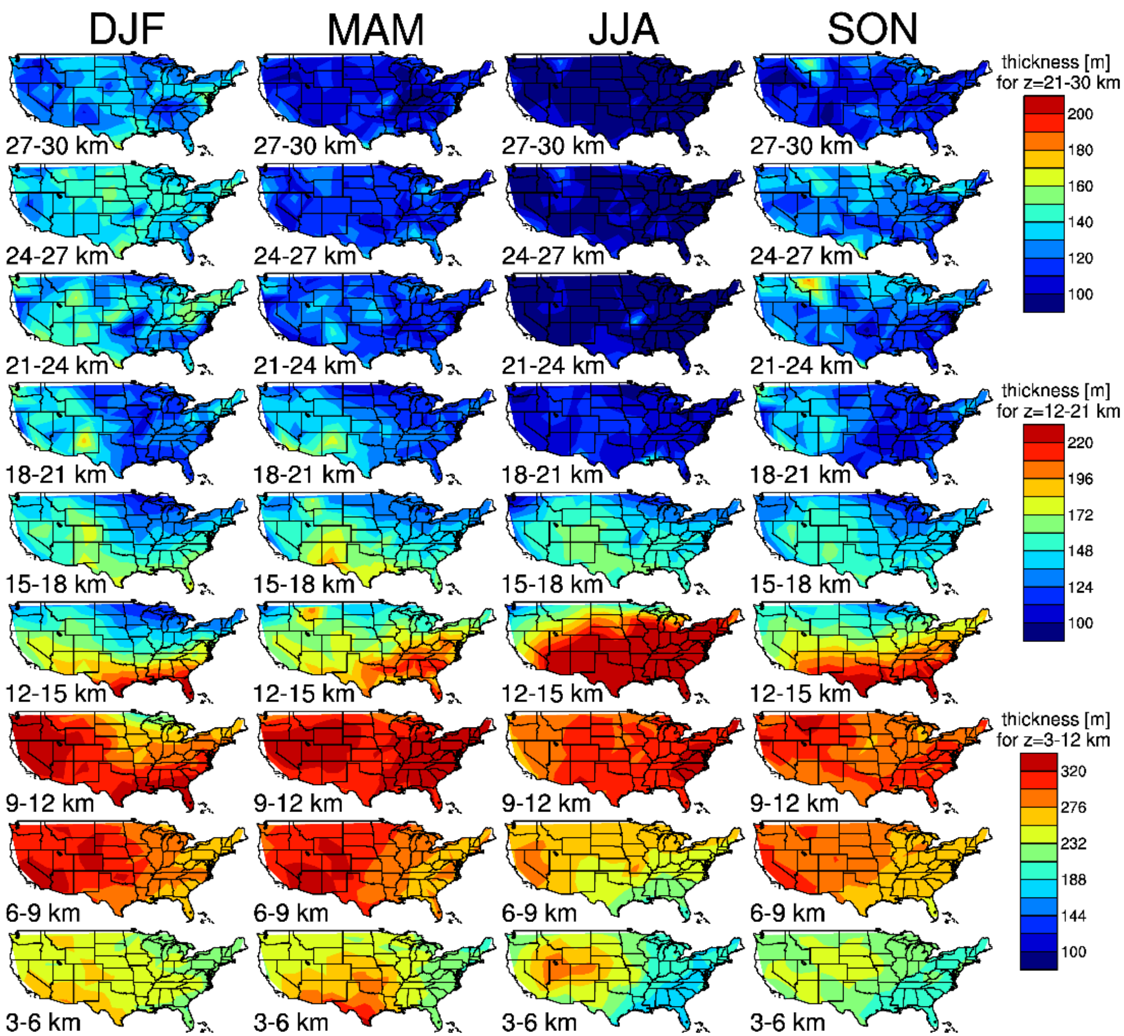

- Layer-mean THTL increases as altitude increases below z=12 km but decreases above z=12 km.
- Below z=12 km, layer-mean THTL is large in DJF and MAM
- Above z=15 km, layer-mean THTL is largest in DJF and smallest in JJA.
- Regionally, at z=3–21 km, layer-mean THTL shows large values in western mountainous region and the southeastern region.

layer-mean THTL = $\frac{\sum \text{THTL}}{n}$, where n is the occurrence number of non-zero THTL in each altitude bin

Horizontal distributions of layer-mean $\log_{10}\varepsilon$

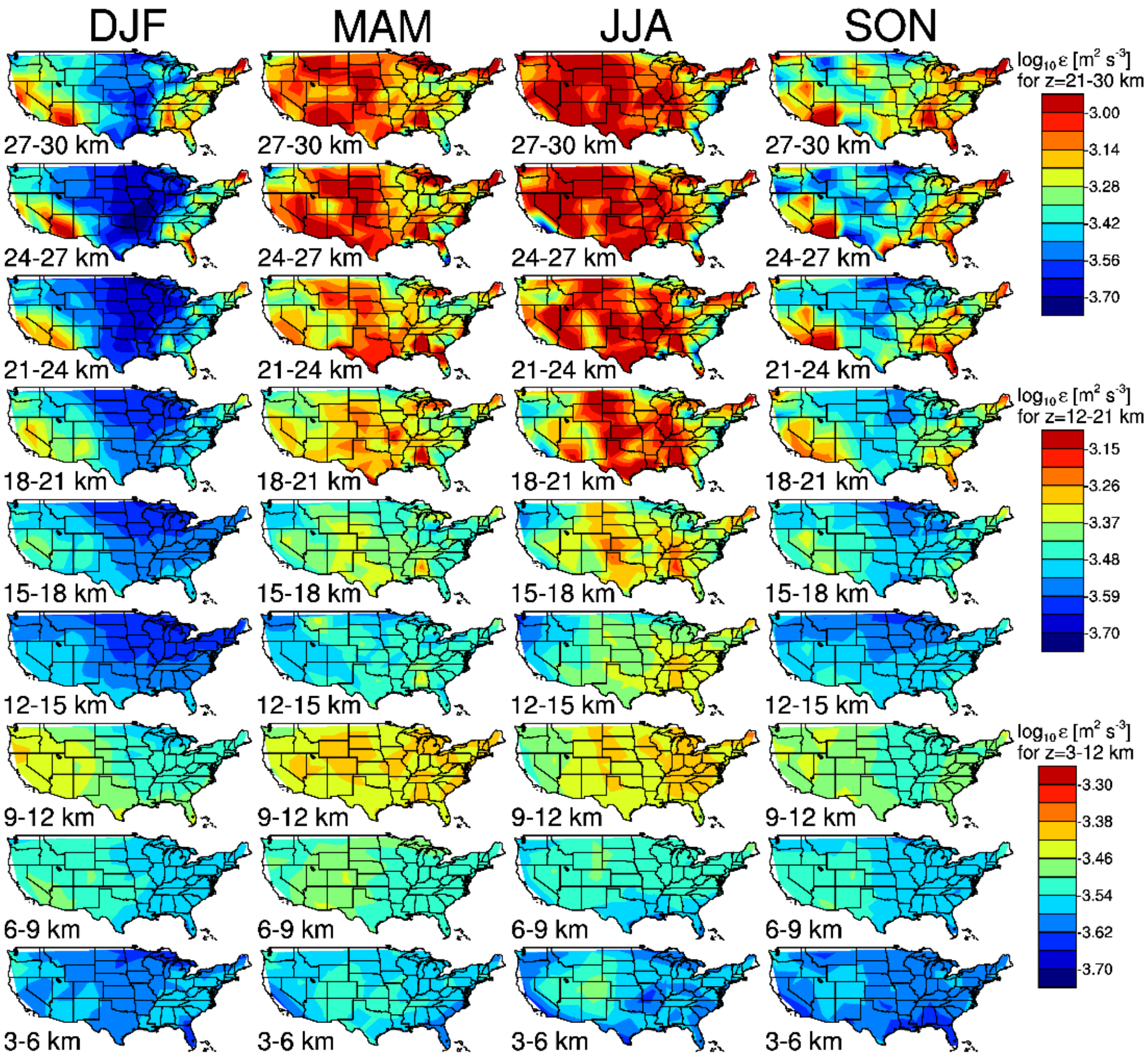

- The seasonal-altitudinal variations of $\log_{10}\varepsilon$ are opposite to those of layer-mean THTL, with large values at high altitudes and in JJA.
- However, the regional pattern is generally consistent with that of the layer-mean THTL
- **Large layer-mean $\log_{10}\varepsilon$ in the high altitudes stems from the smaller number of turbulence cases in the stratosphere than in the troposphere.**

layer-mean $\log_{10}\varepsilon = \frac{\sum \log_{10}\varepsilon}{n}$, where n is the occurrence number of non-zero $\log_{10}\varepsilon$ in each altitude bin

Characteristics of turbulence retrieved from HVRRD

- A simple layer-mean $\log_{10}\varepsilon$ does not properly represent characteristics of turbulence in each layer.
- To better represent the layer-mean turbulence accounting **vertical portion of the turbulence occupation in each bin**, we suggest a new quantity, **the layer-mean effective ε (EE)**, combining turbulence intensity (ε) and the thickness of the turbulence layer (THTL).

Layer-mean effective ε (EE):

$$\frac{\sum \boldsymbol{\varepsilon} \times \mathbf{THTL}}{\boldsymbol{Z}} \qquad [\mathrm{m^2\ s^{-3}}],$$

where $\boldsymbol{Z}$ is the layer depth (3 km in this study) of each altitude bin.

Cf: layer-mean $\log_{10}\varepsilon = \frac{\sum \log_{10}\varepsilon}{n}$, where n is the occurrence number of non-zero $\log_{10}\varepsilon$ in each altitude bin

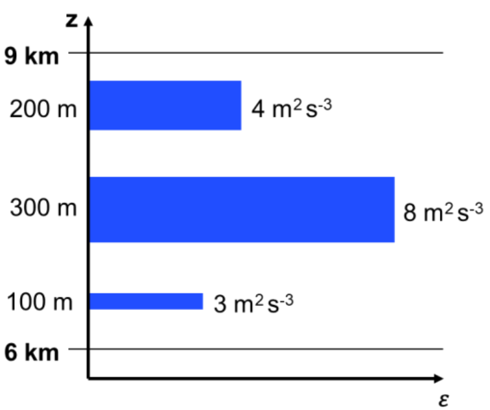

$$\text{EE: } \frac{(3\times100 + 8\times300 + 4\times200 + 0\times2400)\ [\mathrm{m^2\ s^{-3}}][\mathrm{m}]}{3000\ [\mathrm{m}]}$$

Horizontal distributions of EE

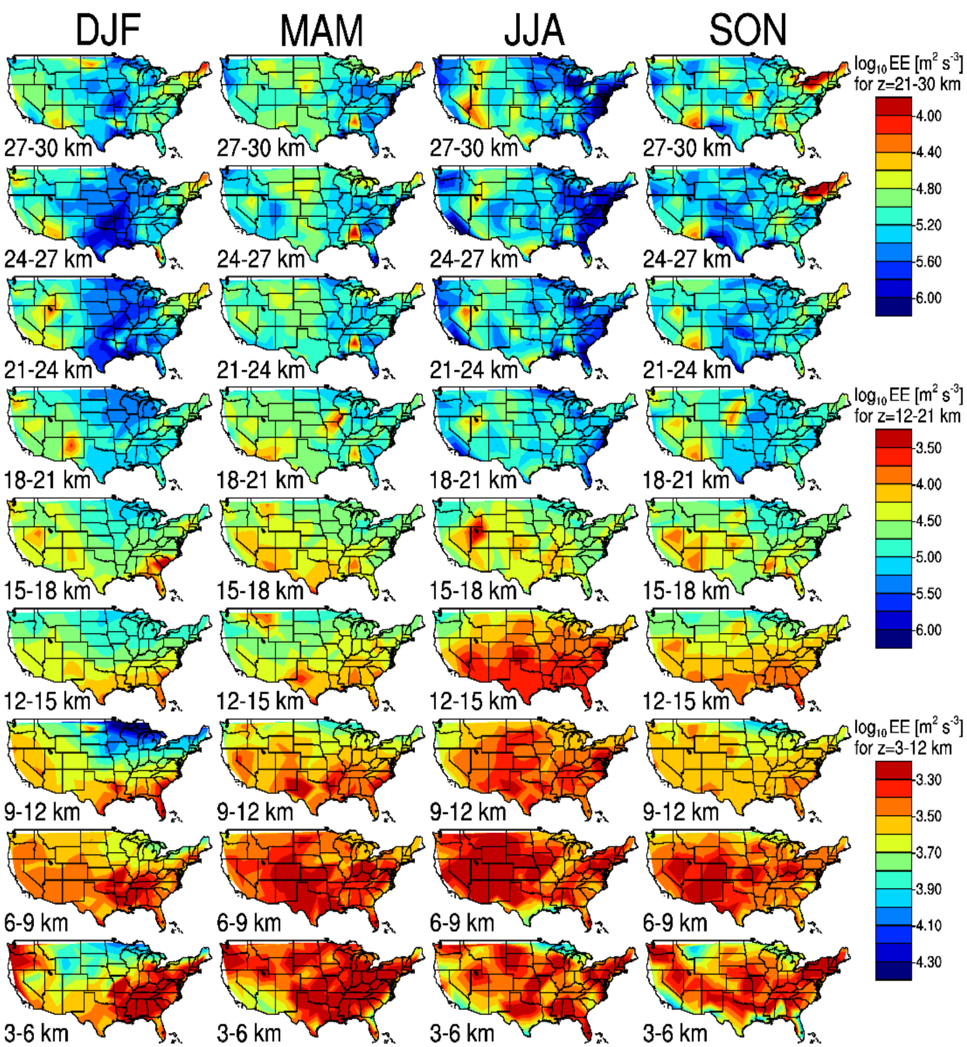

Potential Sources of HVRRD-estimated Turbulence

Turbulence indices are calculated using ERA5 reanalysis

	ERA5 Reanalysis
Horizontal resolution	0.25 x 0.25 [deg]
No. of vertical levels	37 (top: 1 hPa)
Time period	1 hourly
Data period	Jan. 2012-Dec. 2017 (6 years)

Vertical grid spacing of ERA5 Reanalysis

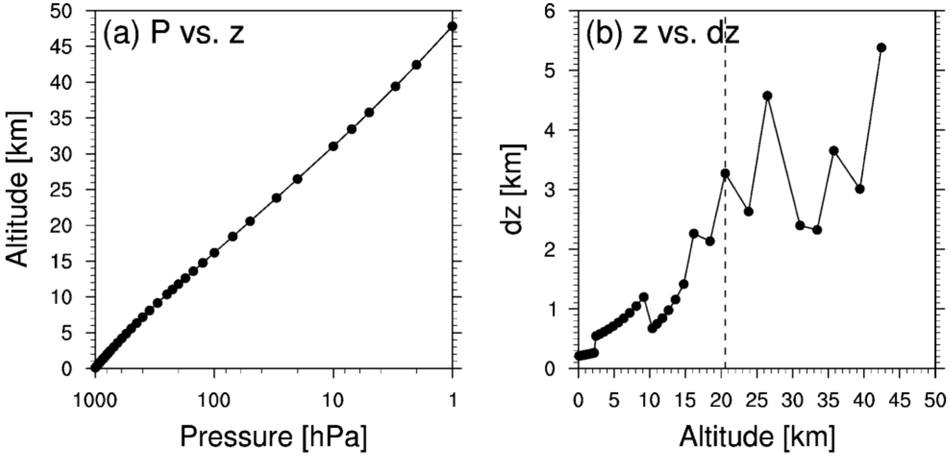

Above ~21 km, vertical grid spacings are ~3 km
→ Results below z=21 km are shown

- Squared Brunt-Vaisala frequency $N^2 = \frac{\theta}{g}\frac{\partial \theta}{\partial z}$
- Vertical wind shear (VWS) $= \sqrt{\left(\frac{\partial u}{\partial z}\right)^2 + \left(\frac{\partial v}{\partial z}\right)^2}$
- Orographic gravity wave drag (OGWD) $= -\frac{1}{\rho}\frac{\partial \tau}{\partial z}$ Palmer et al. (1986), Chun et al. (1996)
- Convective precipitation

Potential Sources (Ko et al. 2019, JGR)

Troposphere (3 km – tropopause)

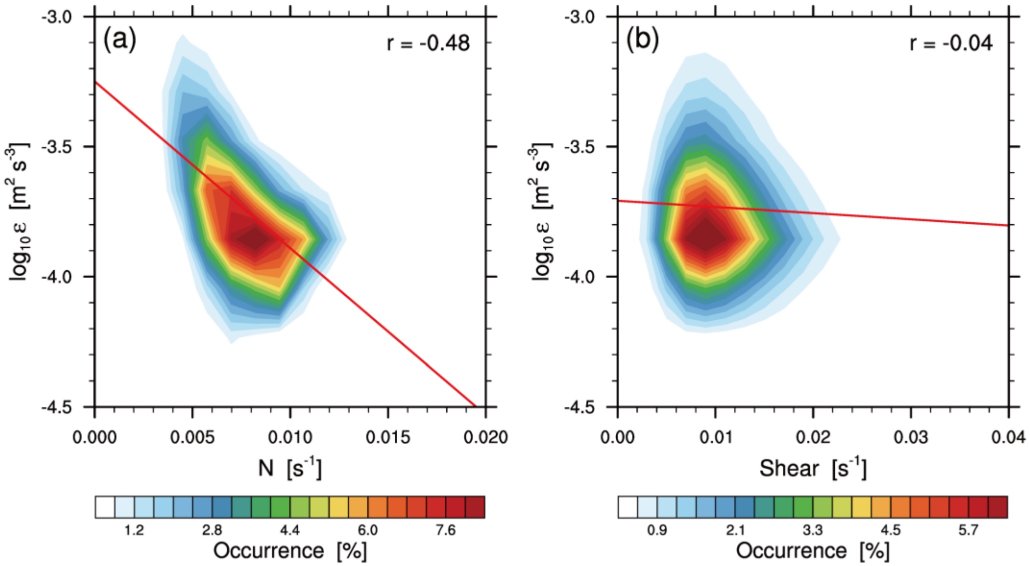

Stratosphere (tropopause – 30 km)

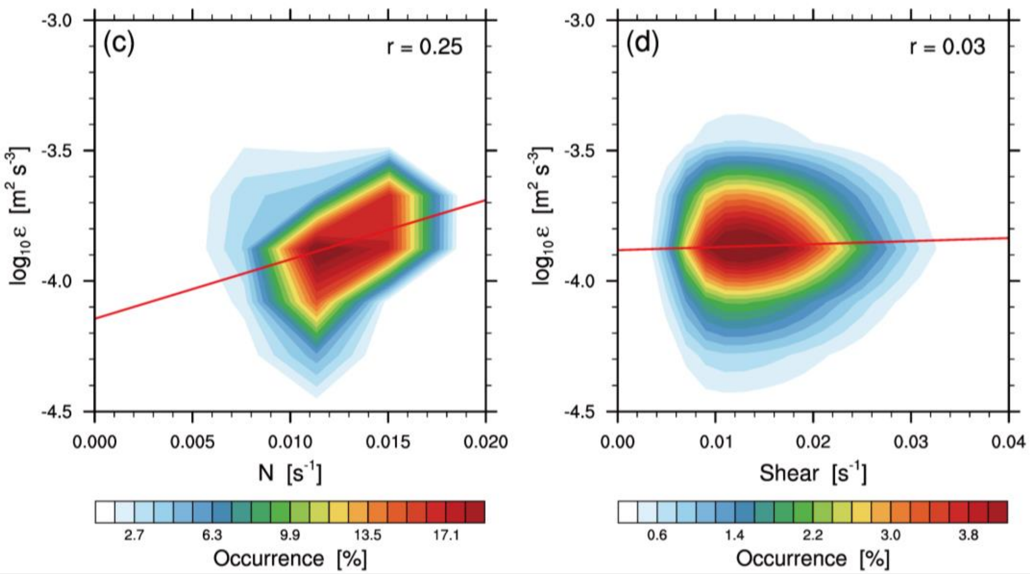

Ko et al. (2019, JGR) r: linear regression coefficient

All 68 station data for 4 years (Sep. 2012-Aug. 2016)

$$\varepsilon = C_K {L_T}^2 N^3$$

- **In the troposphere (a),** the lower the stability, the larger the L_T, and the larger L_T results in a large ε.
  → negative correlation of ε and N
- **In the stratosphere (c),** L_T is relatively small: the larger N, the larger ε.
  → positive correlation of ε and N
- **Correlation between ε and VWS is nearly zero in the TR and ST, likely due to mixing in the turbulence layer**
  → It is difficult to examine potential sources of turbulence using the radiosonde data that include turbulence mixing

Horizontal Distributions of Turbulence Indices

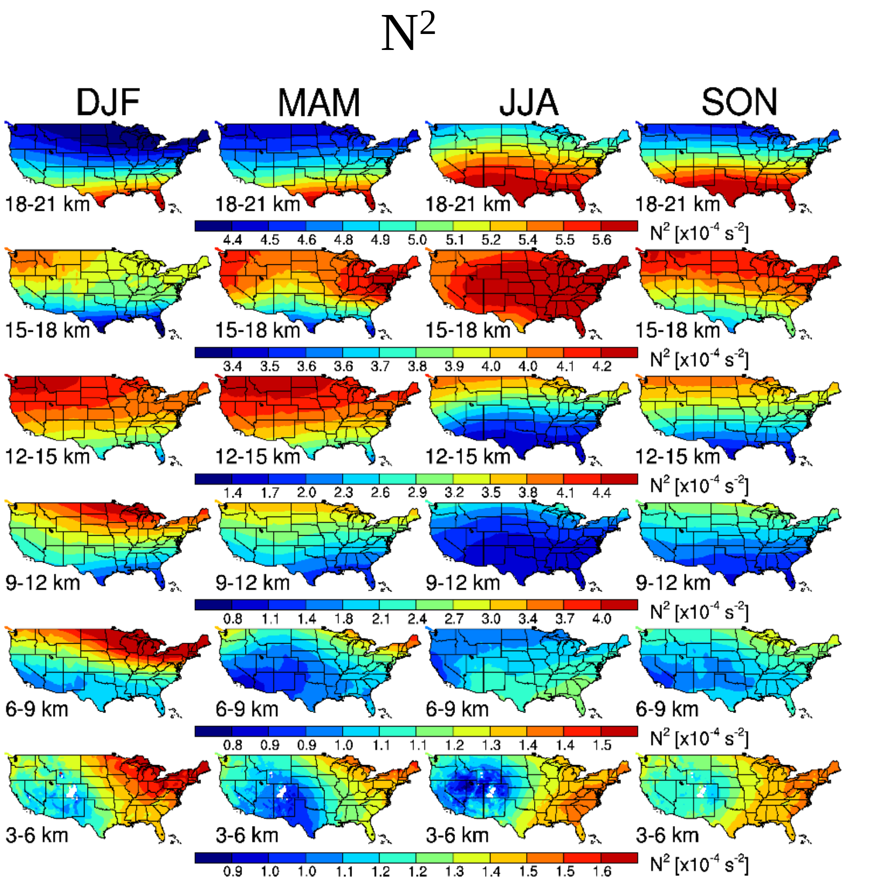

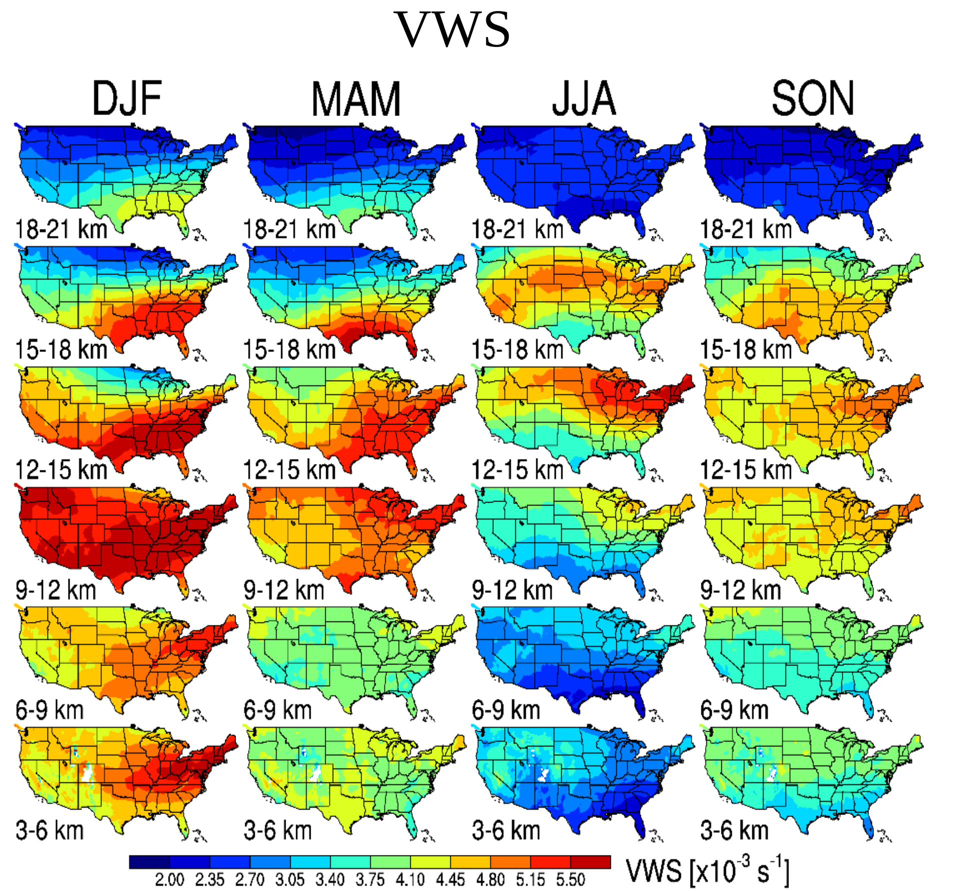

- At z = 3–6 km, weak in western mountain regions, especially in JJA.
- At z = 6–15 km, latitudinal variations are dominant and weak in JJA.
- At z = 18–21 km, strong at low latitudes because the latitudinal temperature structure is opposite to that below in the mid-latitudes (Holton, 2004).

- Large values appear in Eastern USA in most altitudes and seasons, with largest in DJF at z=9–12 km, which can be attributed to the strong jet stream in the Eastern United States (Koch et al., 2006).
- At z = 18–21 km, VWS is much smaller than that below, due to small vertical variation of the large-scale wind in the mid-latitude stratosphere (Holton, 2004).

Horizontal Distributions of Turbulence Indices

OGWD

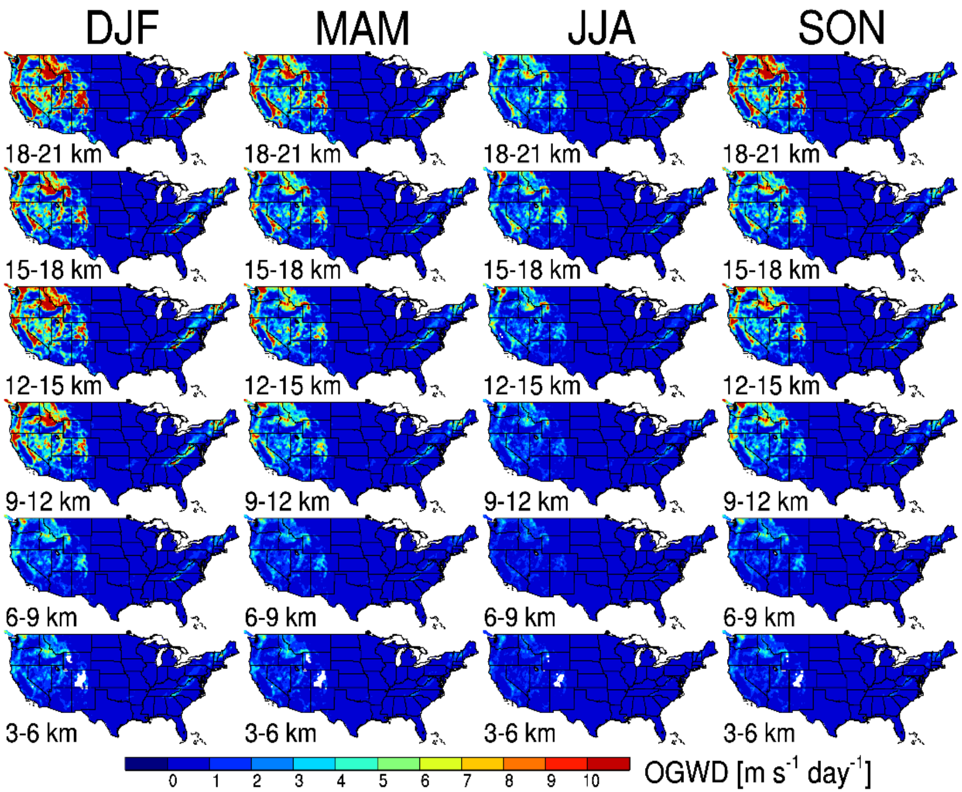

Convective precipitation

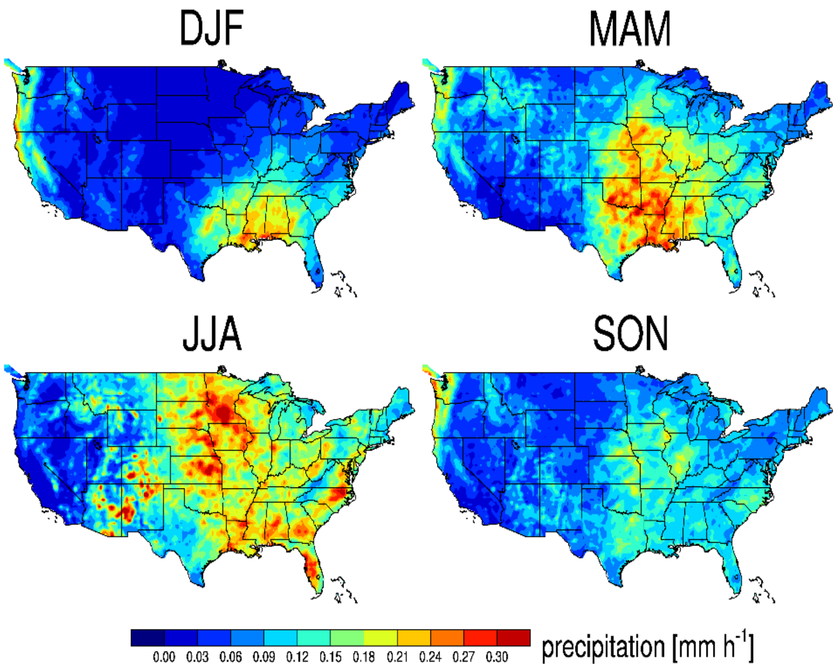

- Stronger OGWD appears in western mountain regions with secondary peaks near eastern mountain regions.
- OGWD shows a clear seasonal variations, largest in DJF and smallest in JJA, and intensity of OGWD increases with altitude, as expected.

- Convective precipitation is largest in JJA throughout the Eastern United States.
- Strong convective precipitation in the west coast of the United States in DJF, MAM, and SON.

Correlation between Monthly-Mean EE and Turbulence Indices

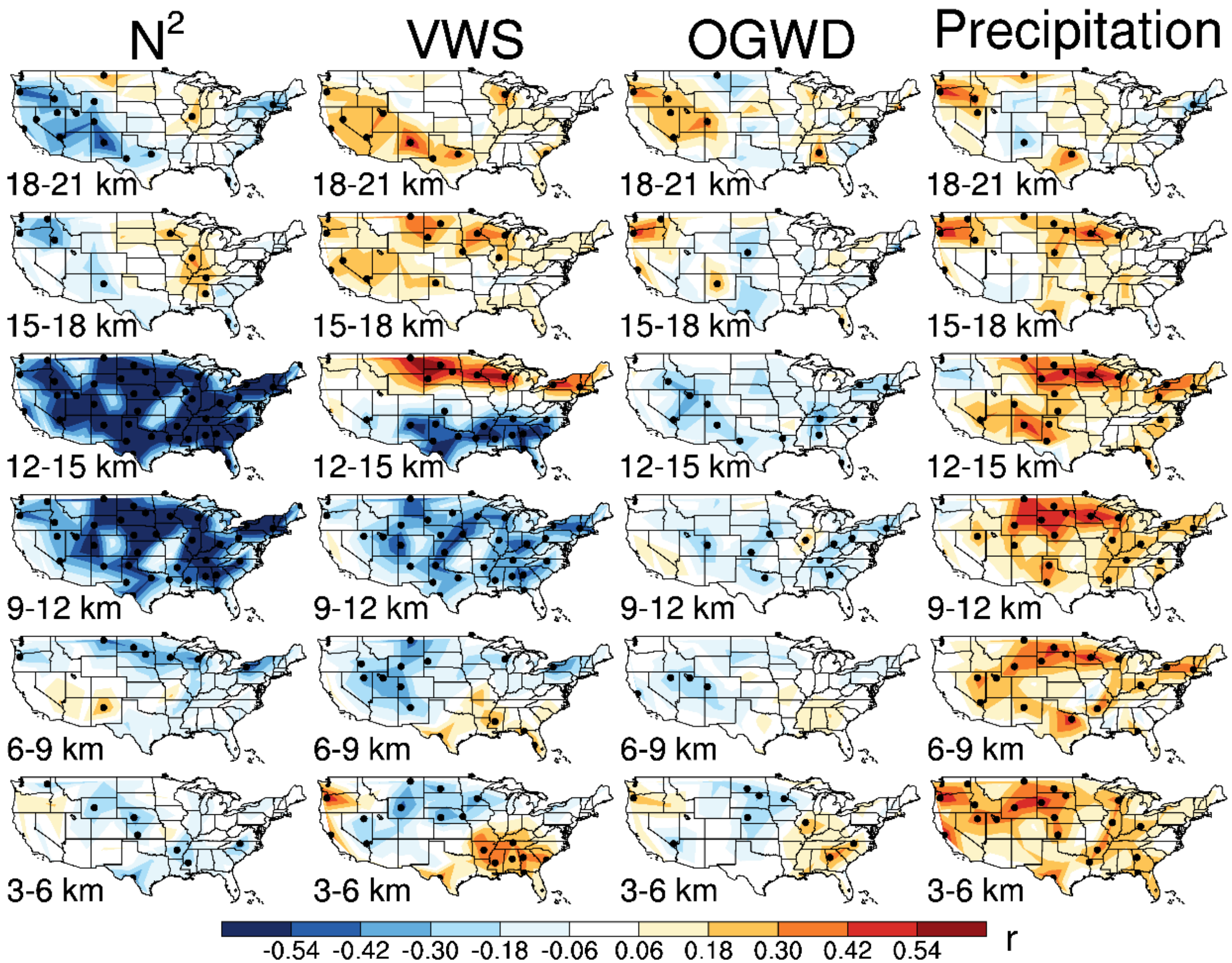

dot: the stations for which the r is significant at the 95% confidence level.

- In most regions, EE and N^2 (Precipitation) are negatively (positively) correlated.
- VWS and OGWD are correlated with EE under specific conditions and in certain locations: VWS is positively correlated under the strong stability and OGWD is positively correlated in western mountain regions at z = 15–21 km.

Comparison of EDRs from HVRRD and Flight Data

Ko et al. (2021, preparing)

■ **In-situ flight EDR Data:** 6 years (Jan. 2012–Dec. 2017) provided from NCAR (Dr. Sharman), with total number of 246,675,712:

- United Airlines B757: 31,818,318
- Delta Air Lines B737 / 767 / 777: 83,382,364 / 67,832,125 / 1,966,538
- Southwest Airlines B737: 61,676,367

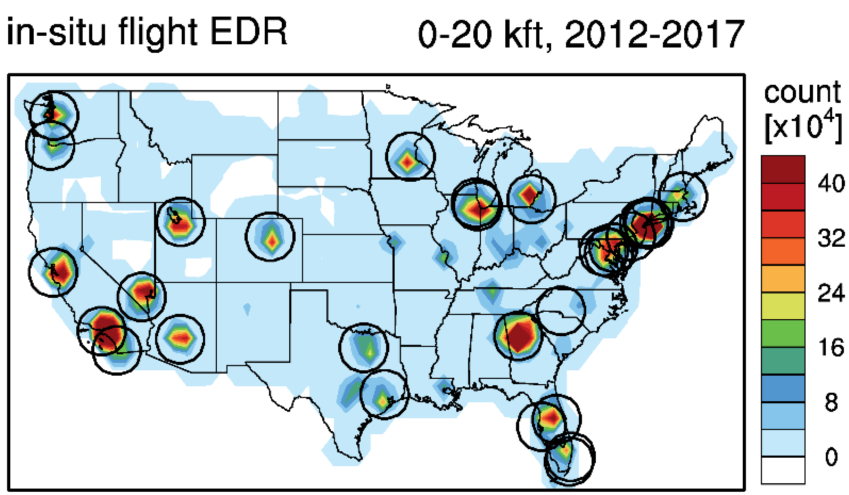

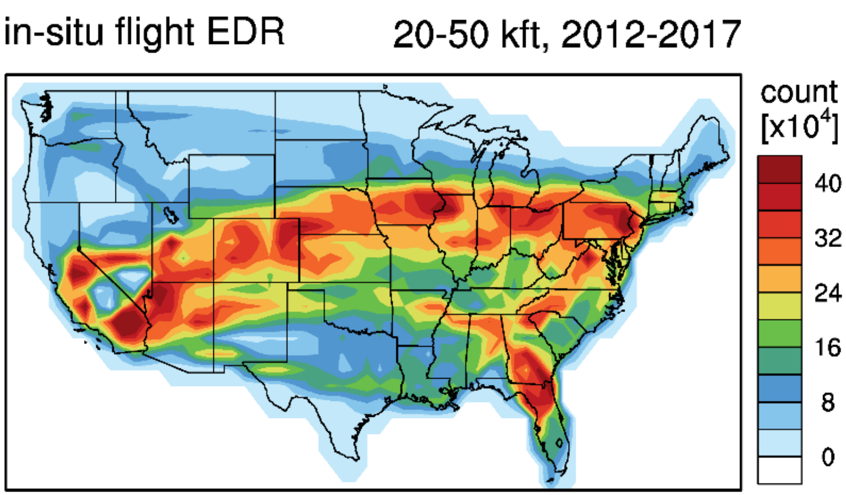

(left) Circles represent locations of top 30 busiest U.S. airports by total passenger boardings (FAA, CY 2017 Passenger Boarding Data).

Comparison in EDRs from HVRRD and Flight Data

2012.1-2017.12
(6 years)

(a) Total counts (z=20–50 kft)

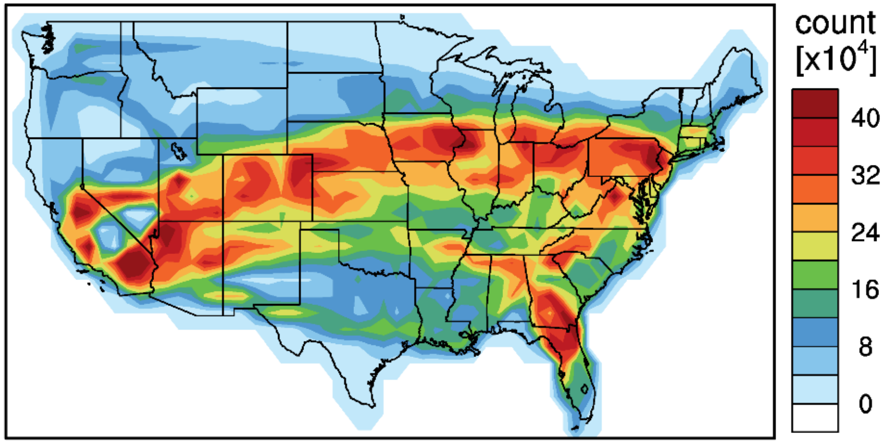

(b) ±1 hours from 00 and 12 UTC

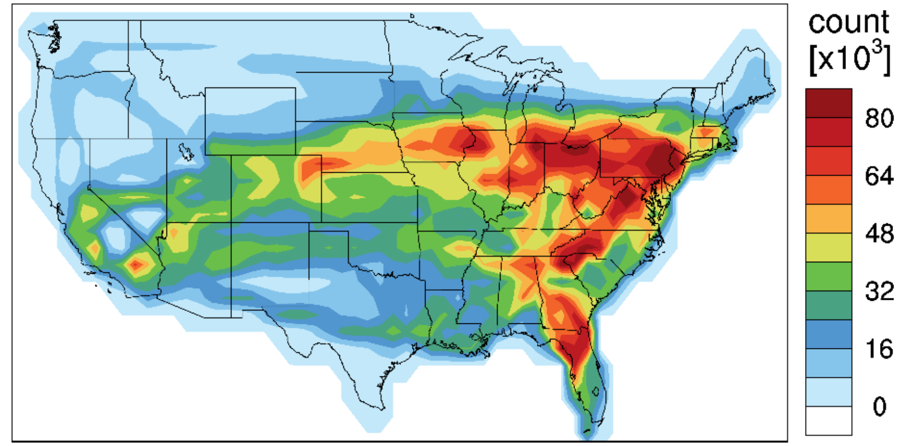

(c) Main flight route

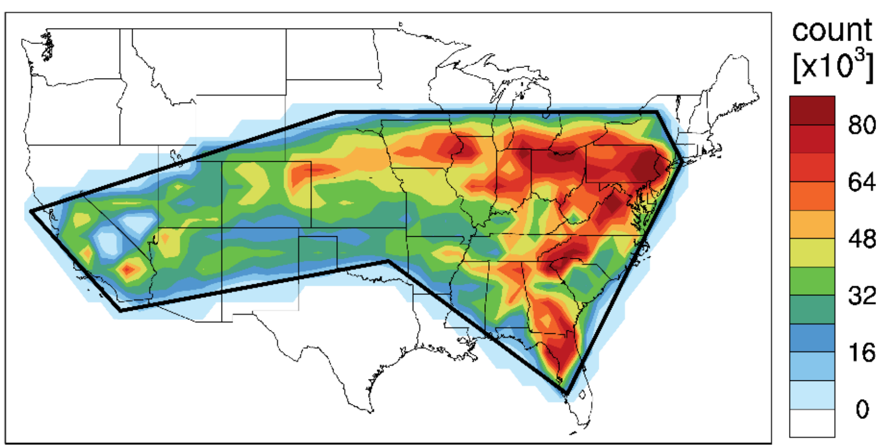

(d) HVRRD stations within main flight route

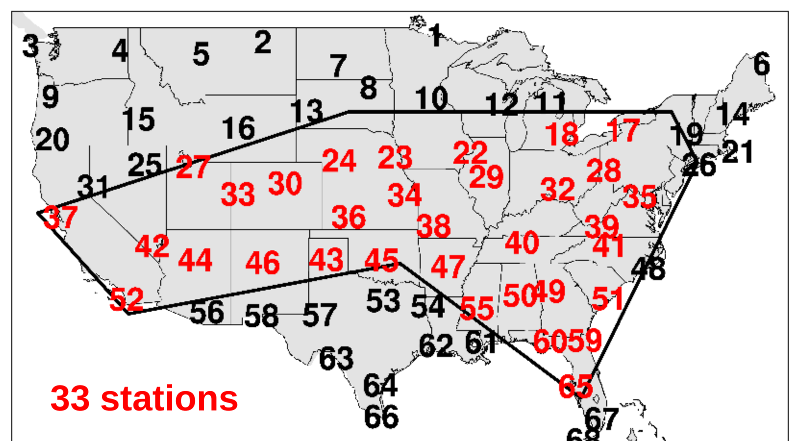

Comparison of EDRs from HVRRD and Flight Data

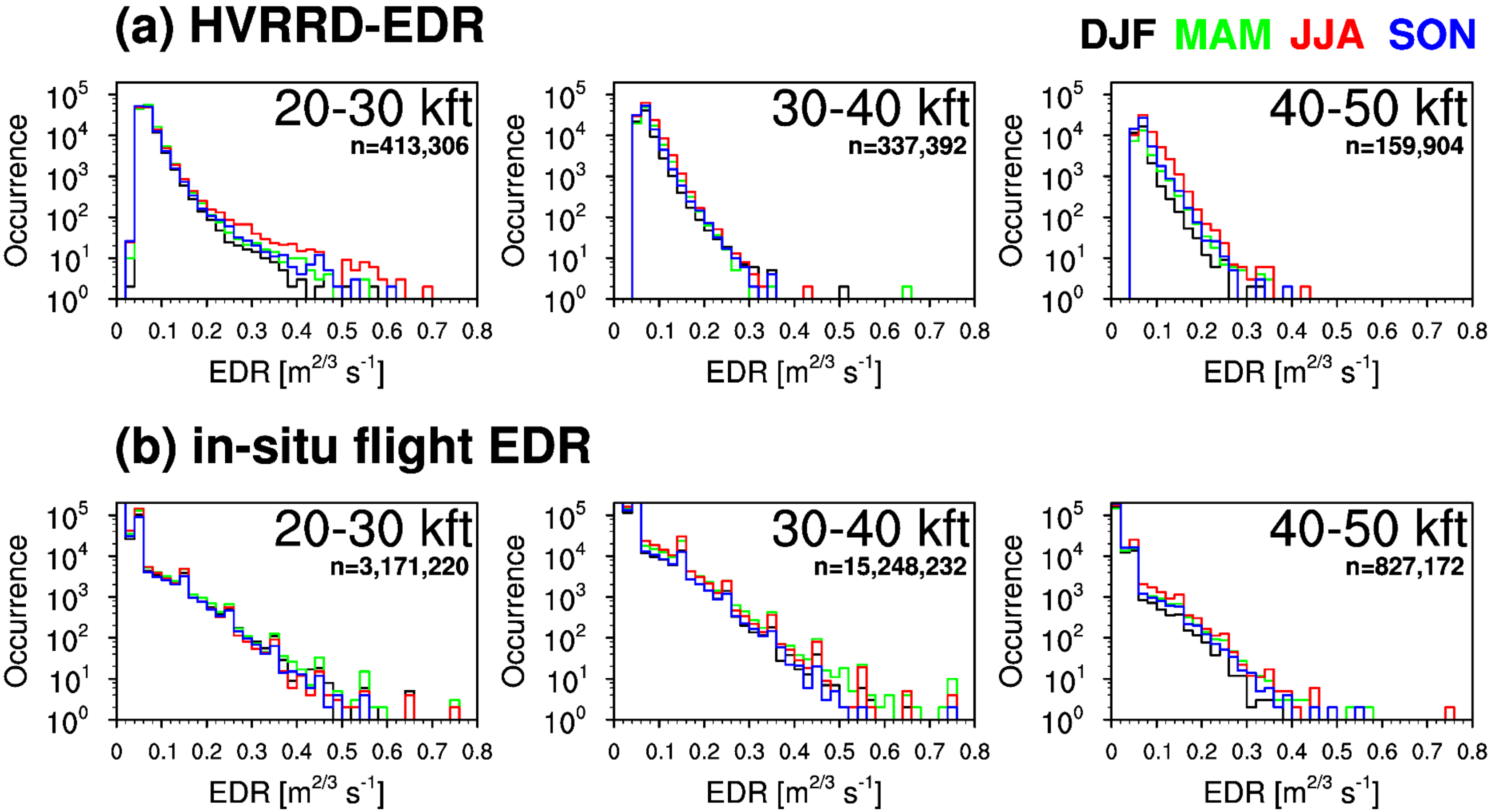

n: total occurrence number in each altitude range

- The maximum of HVRRD-EDR is comparable to flight-EDR at z=20–30 kft, but smaller at z=30–50 kft.
- Both datasets show similar seasonal variations (largest in JJA and smallest in DJF in most altitudes).
- Observed minimum values of L_T=7.1 m and N=0.001851 s^{-1} in HVRRD data→ minimum EDR(=$\varepsilon^{1/3}$) of 0.0068 m$^{2/3}$ s^{-1}.

Comparison: Vertical Distribution

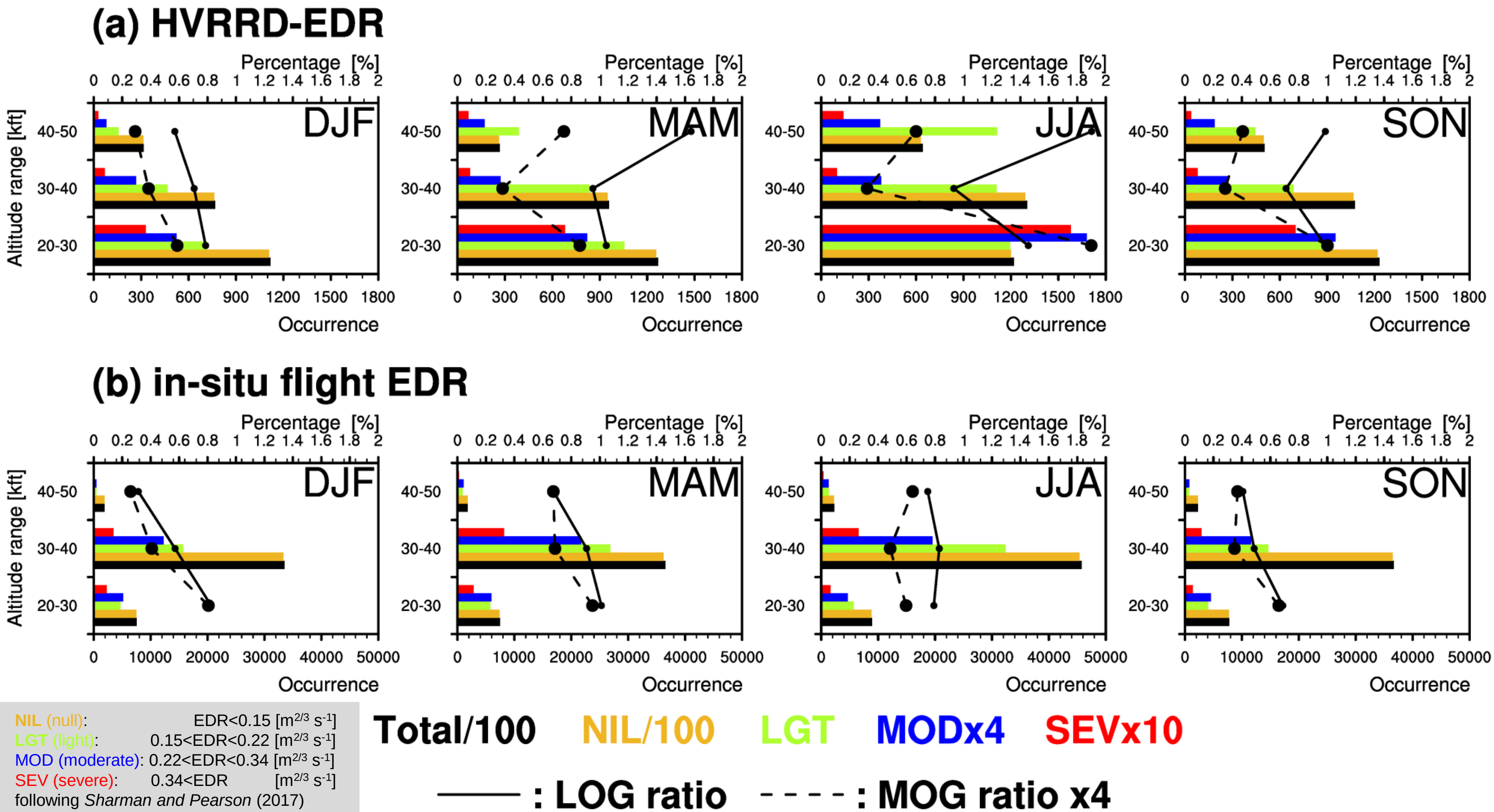

- The vertical distributions of the LOG and MOG ratio of HVRRD-EDR and MOG ratio of in-situ flight EDR show “left angle bracket” shape in MAM, JJA, and SON, but the LOG ratio of in-situ flight EDR decreases in vertical.

Comparison: Horizontal Distribution of LOG Ratio

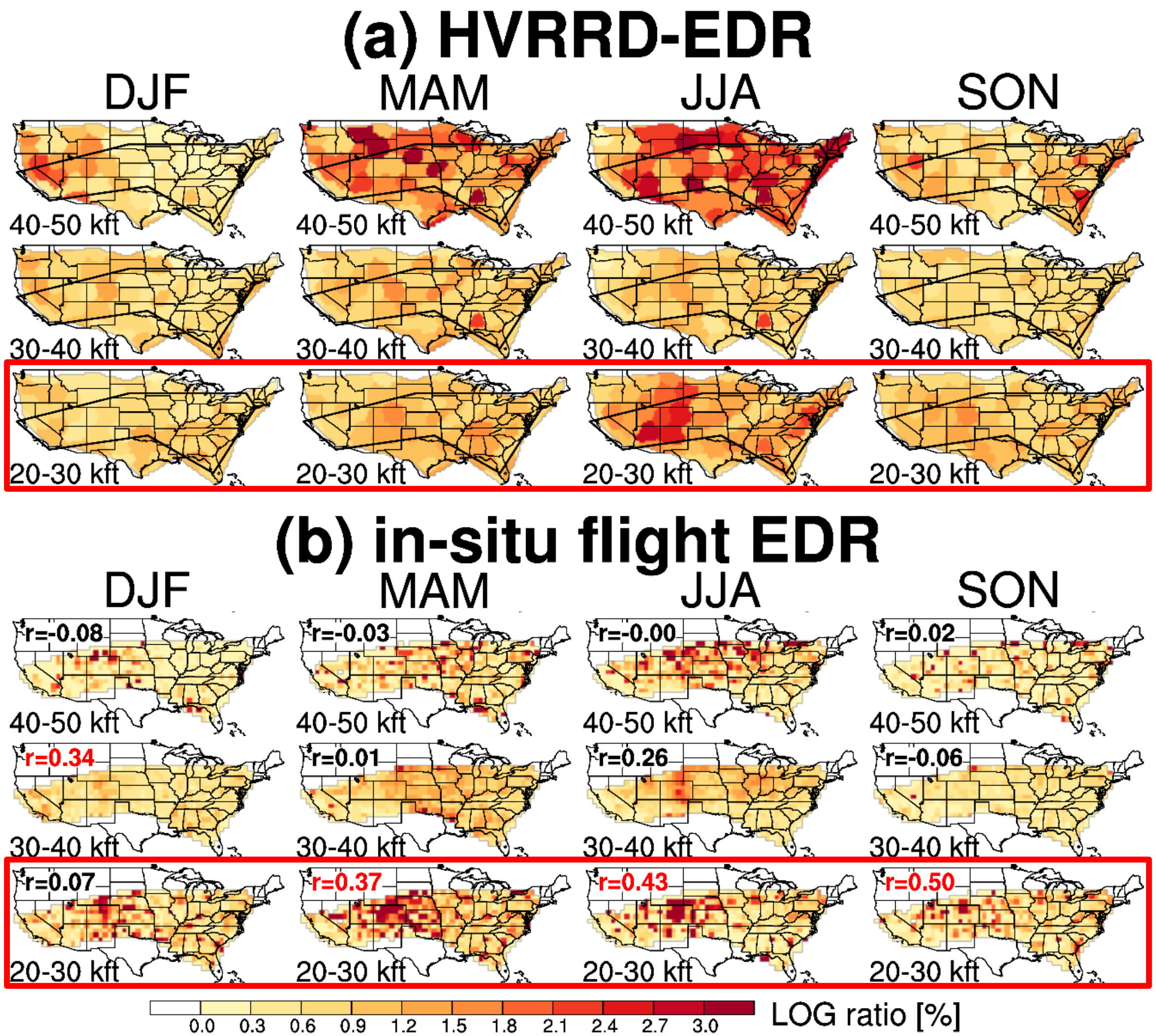

r: pattern correlation coefficient between HVRRD-EDR and flight-EDR, red color represents the significant value at the 95% confidence level

z=40–50 kft

- Local maximum between Nevada and California in DJF, northern and eastern Kansas, and Alabama in MAM, northern Texas, western Nevada, Utah, and Arizona in JJA, with nearly no pattern correlation between HARRD and flight EDRs

z=30–40 kft

- Large LOG ratio in Rocky Mountains, Nevada, and California in DJF, and Colorado, Kansas, Missouri, and Alabama in MAM and JJA, with a significant pattern correlation only in DJF.

z=20–30 kft

- Large LOG ratio around the Rocky mountains and eastern Appalachia mountains, with significant (95%) pattern correlation in all season except in DJF.

Comparison: Horizontal Distribution of LOG Ratio

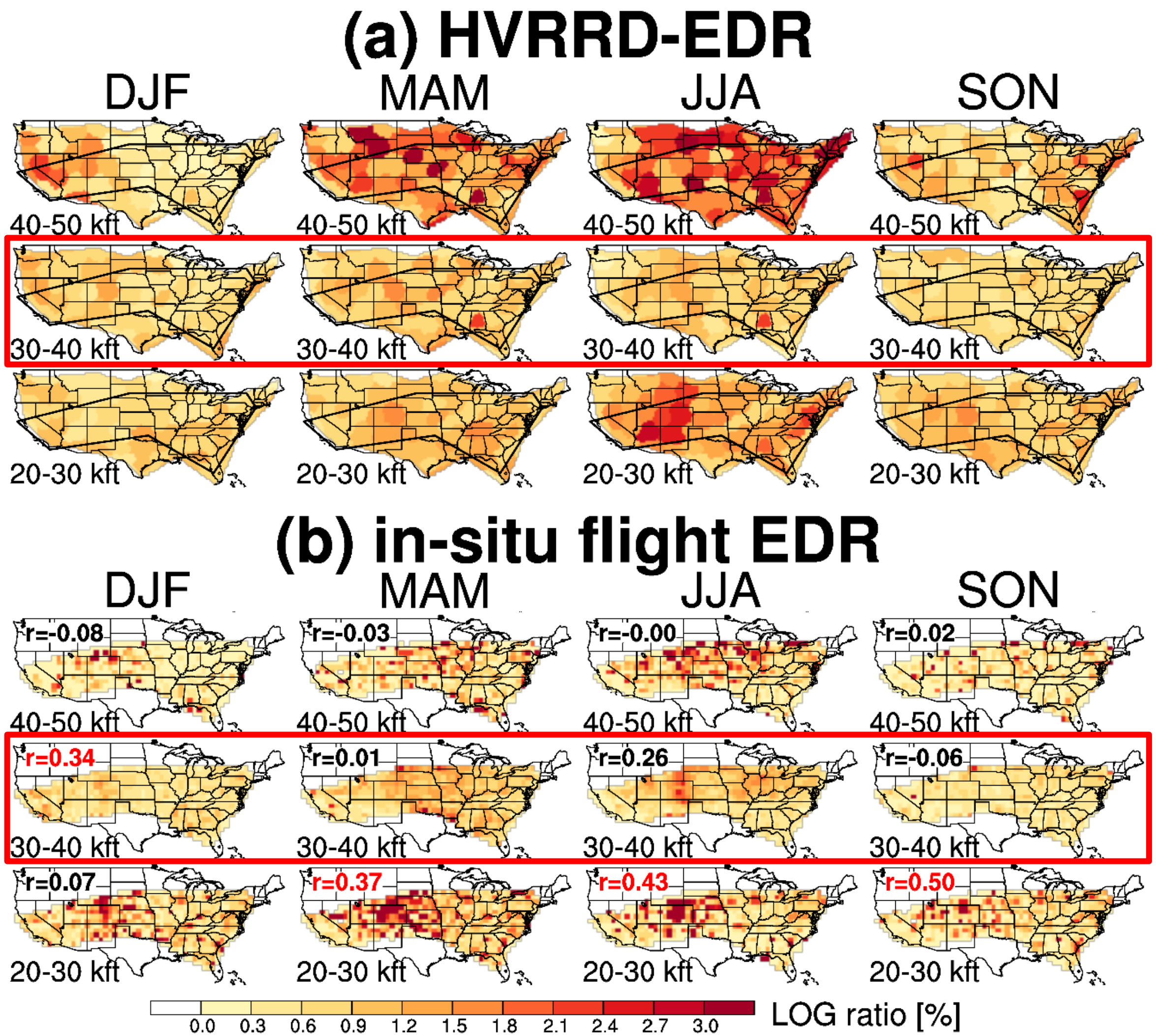

r: pattern correlation coefficient between HVRRD-EDR and flight-EDR, red color represents the significant value at the 95% confidence level

z=40–50 kft

- Local maximum between Nevada and California in DJF, northern and eastern Kansas, and Alabama in MAM, northern Texas, western Nevada, Utah, and Arizona in JJA, with nearly no pattern correlation between HARRD and flight EDRs

z=30–40 kft

- Large LOG ratio in Rocky Mountains, Nevada, and California in DJF, and Colorado, Kansas, Missouri, and Alabama in MAM and JJA, with a significant pattern correlation only in DJF.

z=20–30 kft

- Large LOG ratio around the Rocky mountains and eastern Appalachia mountains, with significant (95%) pattern correlation in all seasons except in DJF.

Comparison: Horizontal Distribution of LOG Ratio

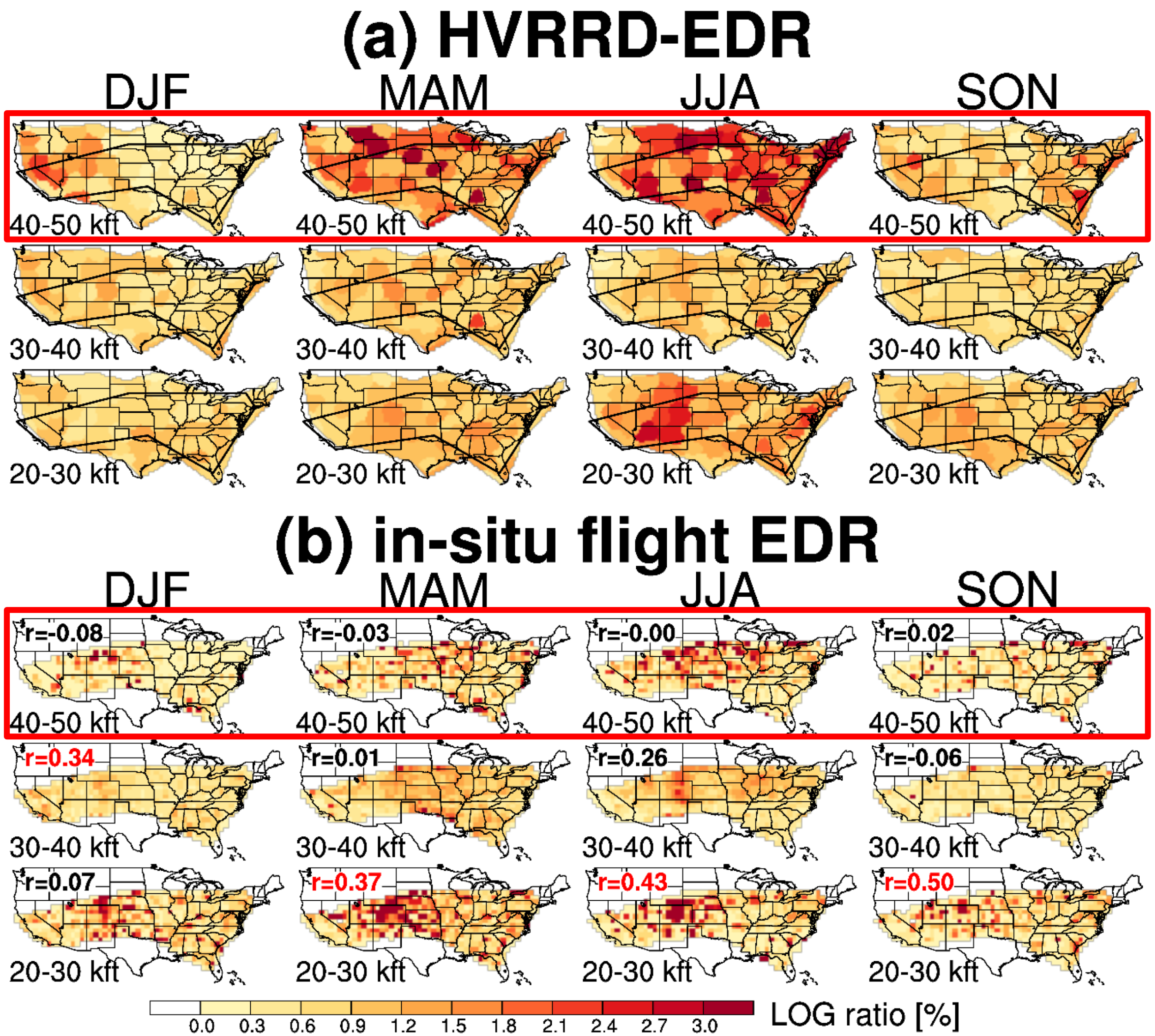

r: pattern correlation coefficient between HVRRD-EDR and flight-EDR, red color represents the significant value at the 95% confidence level

z=40–50 kft

- Local maximum between Nevada and California in DJF, northern and eastern Kansas, and Alabama in MAM, northern Texas, western Nevada, Utah, and Arizona in JJA, with nearly no pattern correlation between HARRD and flight EDRs

z=30–40 kft

- Large LOG ratio in Rocky Mountains, Nevada, and California in DJF, and Colorado, Kansas, Missouri, and Alabama in MAM and JJA, with a significant pattern correlation only in DJF.

z=20–30 kft

- Large LOG ratio around the Rocky mountains and eastern Appalachia mountains, with significant (95%) pattern correlation in all seasons except in DJF.

Comparison: Horizontal Distribution of MOG Ratio

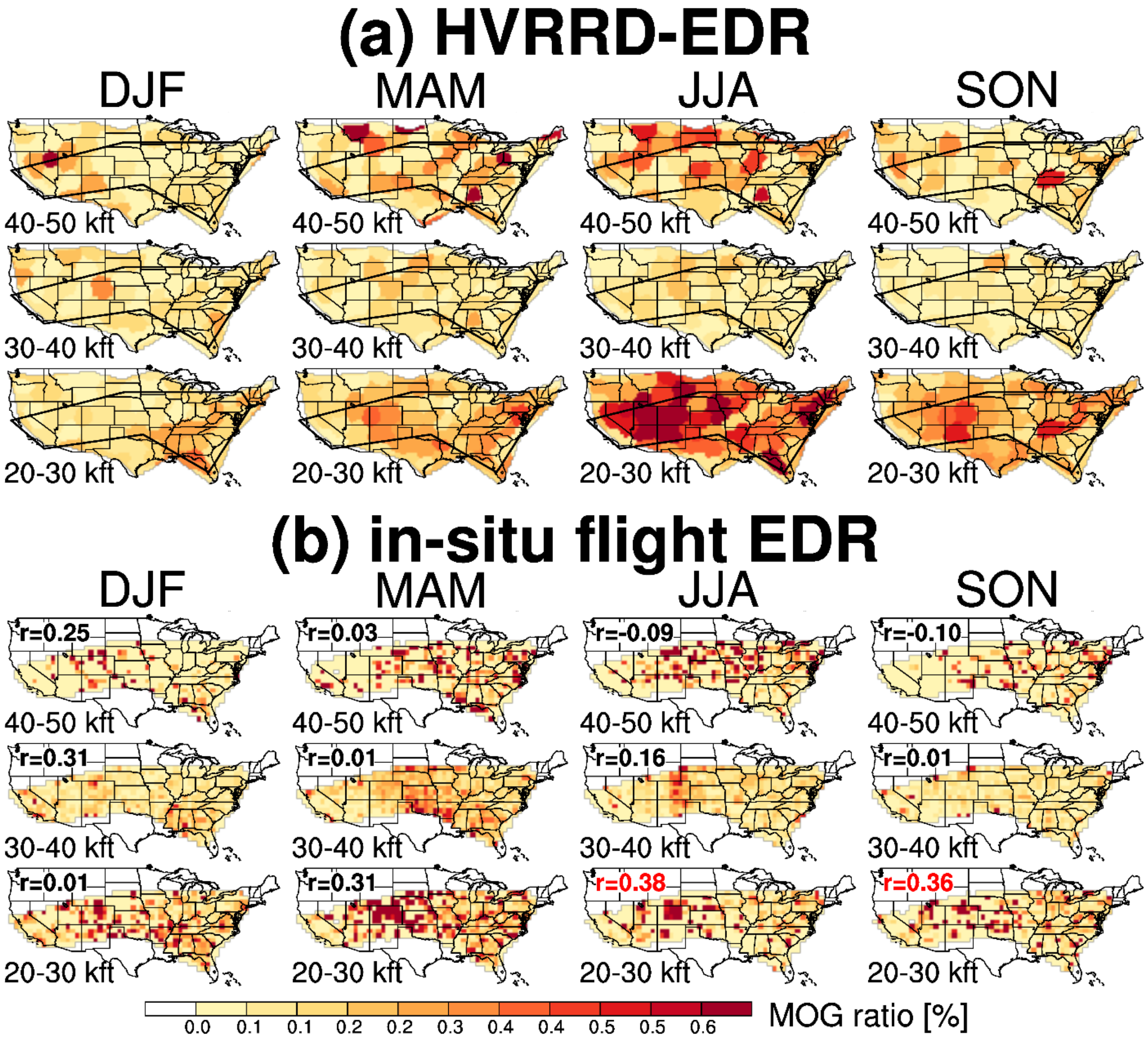

r: pattern correlation coefficient between HVRRD-EDR and flight-EDR, red color represents the significant value at the 95% confidence level

- General features of MOG ratio are consistent with those of LOG ratio.
- Significant (95%) correlation between HVRRD-EDR and flight EDR occurs at 20-30 kft in JJA and SON, with relatively large correlation in MAM at 20-30 kft and DJF at 30-50 kft.

Summary

- We estimated eddy dissipation rate (ε) in the free atmosphere based on Thorpe (1977) method, using **1-s high vertical-resolution radiosonde data (HVRRD) for 6 years (Jan. 2012–Dec. 2017) in USA.**

- **Potential sources of turbulence** are examined by analyzing four turbulence indices calculated using **ERA5 reanalysis data**: N^2, VWS, OGWD, and convective precipitation. *(Ko and Chun 2021, AR)*

- EDR($=\varepsilon^{1/3}$)s derived from HVRRD and in-situ flight data are compared.
  - Vertical distribution of the MOG ratio and horizontal distribution of **LOG and MOG ratios of HVRRD-EDR and in-situ flight EDR are generally consistent with each other, with significant pattern correlation in LOG ratio at 20-30 kft**

- **EDR estimated from HVRRD can be invaluable resource** for atmospheric turbulence research, including aviation turbulence community, which **can be globally available in near future** as more operational radiosondes archive 1-s data.

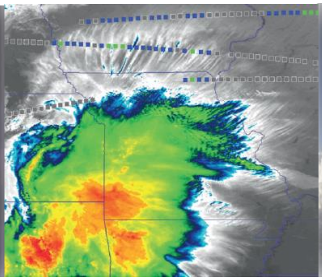

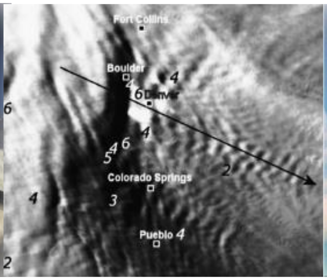

Thank you for your attention!

chunhy@yonsei.ac.kr